Polarization of atomic bremsstrahlung in coincidence studies

Robert A. Müller,[1,2] Vladimir A. Yerokhin,[3] and Andrey Surzhykov[1]
[1]*Helmholtz-Institute Jena, 07743 Jena, Germany*
[2]*Friedrich-Schiller-Universität Jena, 07743 Jena, Germany*
[3]*Saint-Petersburg State Polytechnical University, St. Petersburg 195251, Russia*
(Received 11 July 2014; published 5 September 2014)

We present a theoretical study of bremsstrahlung produced by high-energy electrons scattered by heavy atomic targets. Considering coincident observation of the emitted photons and the scattered electrons, we pay special attention to the polarization degree and direction of the outgoing light. To investigate these properties of atomic bremsstrahlung, we apply the density matrix approach and solutions of the Dirac equation. Detailed calculations are performed for initial electron energies ranging from 100 to 500 keV and different fixed electron scattering angles. The results of these calculations are compared with predictions obtained under the assumption that the scattered electrons remain unobserved. This comparison reveals that both the degree and the direction of linear polarization of bremsstrahlung are very sensitive to the direction of the scattered electron.

DOI: 10.1103/PhysRevA.90.032707 PACS number(s): 34.80.Nz, 41.60.−m, 78.70.En

I. INTRODUCTION

The deceleration of an electron in the field of an atom or ion accompanied by the emission of a photon is called *atomic* or *ordinary* bremsstrahlung if the dynamic response of the target electrons is neglected. As atomic bremsstrahlung is one of the fundamental processes in atomic physics, it has been studied for several decades. Most of the studies of atomic bremsstrahlung in the past were dedicated to the properties of the emitted photons, while the scattered electrons remained unobserved. In these works, the angular distribution of the emitted radiation [1–6] and its polarization [7–9] was investigated. Due to experimental limitations, less attention was paid to setups where the emitted photons and the scattered electrons are observed in coincidence. First steps towards such coincidence experiments were made by Aehlig *et al.* [10,11] and Mergl *et al.* [12] and were reviewed by Nakel [13]. In these experiments, the angular distribution of bremsstrahlung was measured for a fixed electron scattering angle. Theoretical predictions for this kind of experiment were given by Keller and Dreizler [14], Shaffer *et al.* [15], and Tseng [16]. However, with recent developments in solid-state detectors [17–19], not only the angular distribution of bremsstrahlung photons but their polarization becomes accessible in $(e,e'\gamma)$ coincidence experiments. To support and guide such future experiments, which are currently planned at the University of Heidelberg, we present a theoretical analysis of the polarization properties of bremsstrahlung under the assumption that the scattered electrons are observed under a fixed angle. When combined with the (future) experimental data, our predictions will help to better understand the dynamics of the electron spin and its coupling to the orbital momentum in the presence of extremely strong electromagnetic fields. The $(e,e'\gamma)$ coincidence setup favors the study of these electron spin and spin-orbit effects, since it allows one to choose the geometry of the bremsstrahlung process under which the relativistic and magnetic interaction phenomena become of paramount importance.

Before we present the theory for the description of the bremsstrahlung polarization in coincidence experiments, we briefly define in Sec. II the geometry chosen for our discussion of the $(e,e'\gamma)$ process. In Sec. III, we derive the density matrix of the emitted photons. We continue our discussion relating the photon density matrix to the triple-differential cross section of the process and the polarization properties of the emitted photons.

Even though the derived formulas allow for the treatment of any kind of $(e,e'\gamma)$ studies, we apply them first to explore the angular distribution of bremsstrahlung radiation measured in coincidence with the outgoing electrons. For this scenario, we compare our predictions with previous theoretical and experimental results. The polarization properties of the emitted photons are discussed in Sec. IV B. Here we focus on the high-energy part of the spectrum, where the photon gains almost all energy from the incident electron, the *tip region*. This links our investigations to current experimental studies [9,20]. A summary of our results and an outlook are given in Sec. V.

Throughout this paper, atomic units are used ($e = m_e = \hbar = 1$).

II. GEOMETRY OF THE $(e,e'\gamma)$ PROCESS

In this section, we briefly explain the geometry we take as a basis for our discussion of bremsstrahlung, i.e., the scattering of an electron under the simultaneous emission of a photon. It is convenient to describe the properties of bremsstrahlung in the rest frame of the target atom, as shown in Fig. 1. In this frame, the quantization axis (z axis) is chosen along the asymptotic momentum of the incident electron $\boldsymbol{p}_i$. Together with the wave vector $\boldsymbol{k}$, $\boldsymbol{p}_i$ holds the xz plane also referred to as the *emission plane*. Therefore, the direction of the emitted photons is defined by a single angle θ_k. Another plane which we will call the *scattering plane* is defined by the two momentum vectors $\boldsymbol{p}_i$ and $\boldsymbol{p}_f$. Generally, this plane does not coincide with the emission plane. Thus we need two angles, θ_p and φ_p, to characterize the direction of the scattered electrons.

III. THEORY

A. Density matrix of the emitted photons

In the present work, we aim to describe atomic bremsstrahlung for the case of coincident observation of

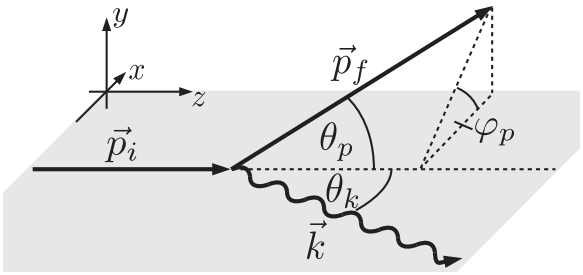

FIG. 1. Geometry of the radiative scattering of an electron by an atom. The z axis is chosen to be along the asymptotic momentum of the incident electron $\boldsymbol{p}_i$. Together with the photon momentum $\boldsymbol{k}$, it defines the xz plane. The angle θ_k is the emission angle of the photon and the angles θ_p and φ_p define the direction of the scattered electron.

the emitted photons and the scattered electrons. Such kind of $(e,e'\gamma)$ coincidence study is performed most naturally by using the density matrix theory. Within this theory, the quantum states of the system before and after the scattering are represented by the *statistical* or *density operator*. For atomic bremsstrahlung, the initial-state statistical operator $\hat{\varrho}_i$ describes the incident electrons with momentum $\boldsymbol{p}_i$ and spin projection m_{s_i}. The operator $\hat{\varrho}_f$, in turn, characterizes the scattered electron $|\boldsymbol{p}_f m_{s_f}\rangle$ and the emitted photon with wave vector $\boldsymbol{k}$ and helicity λ. We can write the matrix of the operator $\hat{\varrho}_f$ in the form

$$\langle \boldsymbol{k}\lambda|\hat{\varrho}_f(\boldsymbol{p}_i,\boldsymbol{p}_f)|\boldsymbol{k}\lambda'\rangle = \sum_{m_{s_i} m'_{s_i} m_{s_f}} \langle \boldsymbol{p}_i m_{s_i}|\hat{\varrho}_i|\boldsymbol{p}_i m'_{s_i}\rangle \times \langle \boldsymbol{p}_i m_{s_i}|\hat{\boldsymbol{\alpha}}\boldsymbol{u}_\lambda e^{i\boldsymbol{kr}}|\boldsymbol{p}_f m_{s_f}\rangle^* \times \langle \boldsymbol{p}_i m'_{s_i}|\hat{\boldsymbol{\alpha}}\boldsymbol{u}_{\lambda'} e^{i\boldsymbol{kr}}|\boldsymbol{p}_f m_{s_f}\rangle, \quad (1)$$

where we assume that the scattered electrons are registered by a polarization-insensitive (electron) detector. Hence we sum over the electron spin projection m_{s_f}, while no integration over the scattering angle Ω_p is performed. This is in contrast to our previous study [21], where the scattered electron remained unobserved.

As seen from Eq. (1), the final-state density matrix depends on the transition amplitudes $\langle \boldsymbol{p}_i m_{s_i}|\hat{\boldsymbol{\alpha}}\boldsymbol{u}_\lambda e^{i\boldsymbol{kr}}|\boldsymbol{p}_f m_{s_f}\rangle$ and the initial-state density matrix $\langle \boldsymbol{p}_i m_{s_i}|\hat{\varrho}_i|\boldsymbol{p}_i m'_{s_i}\rangle$. It is often convenient to express the initial-state density matrix in terms of the so-called *statistical tensor*,

$$\langle \boldsymbol{p}_i m_{s_i}|\hat{\varrho}_i|\boldsymbol{p}_i m'_{s_i}\rangle = \sum_{kq} (-1)^{\frac{1}{2}-m'_{s_i}} (1/2 m_{s_i}\, 1/2 m'_{s_i}|kq)\varrho^{(i)}_{kq}, \quad (2)$$

whose components are directly related to the spin polarization of the incident electrons via the Stokes parameters (cf. Ref. [22]):

$$\varrho^{(i)}_{00} = \frac{1}{\sqrt{2}}, \quad \varrho^{(i)}_{10} = \frac{1}{\sqrt{2}} P_z, \quad \varrho^{(i)}_{1\pm1} = \mp\frac{1}{\sqrt{2}}(P_x \mp \mathrm{i}P_y). \quad (3)$$

Each Stokes parameter P_x, P_y, and P_z characterizes the degree of polarization in a certain direction. The three Stokes parameters together build the *polarization vector* $\boldsymbol{P}_e = (P_x, P_y, P_z)$.

Besides the initial-state density matrix $\langle \boldsymbol{p}_i m_{s_i}|\hat{\varrho}_i|\boldsymbol{p}_i m'_{s_i}\rangle$, the density matrix (1) of the emitted photons also depends on the matrix element $\langle \boldsymbol{p}_i m_{s_i}|\hat{\boldsymbol{\alpha}}\boldsymbol{u}_\lambda e^{i\boldsymbol{kr}}|\boldsymbol{p}_f m_{s_f}\rangle$. Such a matrix element describes a transition between continuum electron states under the simultaneous emission of a photon. The photon is described by a plane wave $\boldsymbol{u}_\lambda e^{i\boldsymbol{kr}}$, while the electrons are described by continuum solutions $|\boldsymbol{p}m\rangle$ of the Dirac equation including an effective atomic potential. The construction of this potential is discussed in Sec. III C. For further evaluation of the transition amplitude, one needs to expand both the continuum wave functions $\langle \boldsymbol{r}|\boldsymbol{p}m_s\rangle$ and the electron-photon interaction operator $\hat{\boldsymbol{\alpha}}\boldsymbol{u}_\lambda e^{i\boldsymbol{kr}}$ into partial waves. Since the partial-wave decompositions of electron and photon waves have been often discussed in the past, we will not show them here explicitly and instead refer the reader to the literature [21,23,24]. Based upon an application of these decompositions and by inserting Eq. (2) into Eq. (1), we find that the final-state density matrix (4) can be expressed as a sum of products of two terms:

$$\langle \boldsymbol{k}\lambda|\hat{\varrho}_f(\boldsymbol{p}_i,\boldsymbol{p}_f)|\boldsymbol{k}\lambda'\rangle = \sum_{bgtkr} \mathrm{K}^{bg}_{tkr}(Z,\varepsilon_i,\varepsilon_f)\Theta^{bg}_{tkr}(\boldsymbol{k},\boldsymbol{p}_f,\boldsymbol{P}_e). \quad (4)$$

The spin-angular function $\Theta^{bg}_{tkr}(\boldsymbol{k},\boldsymbol{p}_f,\boldsymbol{P}_e)$ depends only on the polarization of the incident electrons and the angles of the outgoing particles. It is given by

$$\Theta^{bg}_{tkr}(\boldsymbol{k},\boldsymbol{p}_f,\boldsymbol{P}_e) = \Big[\big[\mathrm{D}^b_0(\boldsymbol{p}_f)\otimes \mathrm{D}^g_{\lambda'-\lambda}(\boldsymbol{k})\big]_t \otimes \varrho^{(i)}_k\Big]_{r0}, \quad (5)$$

where $\mathrm{D}^l_{mm'}(\varphi,\theta,\psi)$ is the Wigner rotation matrix and $[A_a\otimes A_b]_{c\gamma} = \sum_{\alpha\beta}(a\alpha b\beta|c\gamma)A_{a\alpha}B_{b\beta}$. Accordingly, the kinematical coefficients $\mathrm{K}^{bg}_{tkr}(Z,\varepsilon_i,\varepsilon_f)$ are independent of the angular and polarization properties of the process but cover all dependencies on the kinematical parameters, i.e., the energies of the incoming and outgoing electrons and the nuclear charge. Explicitly, they read

$$\begin{aligned}
&\mathrm{K}^{bg}_{tkr}(Z,\varepsilon_i,\varepsilon_f) \\
&= 2^5\pi^{\frac{5}{2}} \sum_{LL'pp'} \sum_{\kappa_i\kappa_f} \sum_{\kappa'_i\kappa'_f} (-i\lambda)^p (i\lambda')^{p'} \\
&\quad\times (-1)^{\frac{1}{2}+2j'_f+j_f-j_i+j'_i-l_i-k+L} \\
&\quad\times i^{L'-L+l'_f-l_f+l_i-l'_i} e^{i(\Delta_{\kappa_i}+\Delta_{\kappa_f}-\Delta_{\kappa'_i}-\Delta_{\kappa'_f})} \\
&\quad\times [j_i,j'_i,j_f,j'_f,l_i,l'_i,l_f,l'_f,L,L',b,g,k,t]^{\frac{1}{2}} \\
&\quad\times (l'_f 0 l_f 0|b0)(l'_i 0 l_i 0|r0)(L'\lambda' L-\lambda|g(\lambda'-\lambda)) \\
&\quad\times \begin{Bmatrix} l'_f & \frac{1}{2} & j'_f \\ j_f & b & l_f \end{Bmatrix} \begin{Bmatrix} L & L' & g \\ j_f & j'_f & b \\ j_i & j'_i & t \end{Bmatrix} \begin{Bmatrix} \frac{1}{2} & \frac{1}{2} & k \\ j_i & j'_i & t \\ l_i & l'_i & r \end{Bmatrix} \\
&\quad\times \langle \varepsilon_i\kappa_i\|\hat{\boldsymbol{\alpha}}\boldsymbol{a}^{(p)}_L\|\varepsilon_f\kappa_f\rangle^* \langle \varepsilon_i\kappa'_i\|\hat{\boldsymbol{\alpha}}\boldsymbol{a}^{(p')}_{L'}\|\varepsilon_f\kappa_f\rangle. \quad (6)
\end{aligned}$$

Here we introduced the symbol $[j_1,j_2,\ldots] = (2j_1+1)(2j_2+1)\ldots$. The summation indices κ_i and κ_f are the relativistic orbital quantum numbers which characterize the multipole components of the initial and final electron states. The corresponding total and orbital angular momenta are given by $j = |\kappa| - 1/2$ and $l = |\kappa + 1/2| - 1/2$. The term $\Delta_\kappa = \sigma_\kappa + \pi/2(l+1)$ is the Dirac phase related to the asymptotic phase σ_κ of the Dirac wave function (see Ref. [21] for

details). Furthermore, the kinematical coefficients (6) depend on the reduced matrix elements $\langle \varepsilon_i \kappa_i \| \hat{\boldsymbol{\alpha}} \boldsymbol{a}_L^{(p)} \| \varepsilon_f \kappa_f \rangle$ for electric ($p = 1$) and magnetic ($p = 0$) transitions with multiplicity L. Their evaluation is sketched in Sec. III C and has been discussed in detail in Ref. [21].

B. Triple-differential cross section and polarization parameters

In the previous section, we derived an expression for the final-state density matrix (4), which depends on the emission angles of both scattered electrons and emitted bremsstrahlung photons. All properties of bremsstrahlung radiation in $(e,e'\gamma)$ coincidence experiments can be expressed in terms of the entries of this matrix. For example, the scaled [16] triple-differential cross section (differential in the photon energy and in the electron scattering and photon emission angles) is given by

$$\frac{d\sigma^3}{dk d\Omega_k d\Omega_p} = \frac{1}{128\pi^2} \frac{k^2}{p_i^2} \frac{\alpha}{Z^2} \sum_{\lambda} \langle \boldsymbol{k}\lambda | \hat{\varrho}_f(\boldsymbol{p}_i, \boldsymbol{p}_f) | \boldsymbol{k}\lambda \rangle, \quad (7)$$

upon summation over the helicity of the outgoing photon. Besides the dependence of the density matrix on the photon and electron energies, the triple-differential cross section is proportional to the square of the factor k/p_i. This quantity describes the momentum of the photon k in units of the incident electron momentum p_i and, hence, it varies in the range from 0 to 1.

In addition to the triple-differential cross section (7), we can also construct the Stokes parameters of the emitted photons from the final-state density matrix. Following Ref. [22], these parameters are defined as

$$\frac{\langle \boldsymbol{k}\lambda | \hat{\varrho}_f(\boldsymbol{p}_i, \boldsymbol{p}_f) | \boldsymbol{k}\lambda' \rangle}{\sum_{\tilde{\lambda}} \langle \boldsymbol{k}\tilde{\lambda} | \hat{\varrho}_f(\boldsymbol{p}_i, \boldsymbol{p}_f) | \boldsymbol{k}\tilde{\lambda} \rangle} = \frac{1}{2} \begin{pmatrix} 1 + P_3 & P_1 - iP_2 \\ P_1 + iP_2 & 1 - P_3 \end{pmatrix}. \quad (8)$$

The third parameter P_3 characterizes the degree of circular polarization. For photon energies in the order of keV, the circular polarization is experimentally very difficult to access, so we focus on the linear polarization which is described by the parameters P_1 and P_2. These are related to the intensity I_Φ of the emitted radiation polarized in an angle Φ with respect to the emission plane (see Fig. 1):

$$P_1 = \frac{I_{0^\circ} - I_{90^\circ}}{I_{0^\circ} + I_{90^\circ}}, \quad (9a)$$

$$P_2 = \frac{I_{45^\circ} - I_{135^\circ}}{I_{45^\circ} + I_{135^\circ}}. \quad (9b)$$

In order to compare theoretical and experimental results, it is more convenient to represent the linear polarization of light in terms of the polarization ellipse. This ellipse is parametrized by its eccentricity P_L, also referred to as *degree of linear polarization*, and the tilt angle χ of its principal axis with respect to the chosen frame, which is commonly called *polarization angle*. The parameters P_L and χ are related to the Stokes parameters as

$$P_L = \sqrt{P_1^2 + P_2^2}, \quad (10a)$$

$$\chi = \frac{1}{2} \arctan \frac{P_2}{P_1}. \quad (10b)$$

In Sec. IV B, we shall discuss how these experimental observables P_L and χ are influenced if the scattered electrons are observed together with the bremsstrahlung photons.

C. Numerical evaluation of the reduced matrix elements

The general formulas given by Eqs. (4) and (6) reduce the problem of calculating the final-state density matrix to the evaluation of the reduced matrix elements of the electric ($p = 1$) and magnetic ($p = 0$) photon emission operator with the Dirac continuum-state wave functions,

$$M_{if}(pL) = \langle \varepsilon_i \kappa_i \| \hat{\boldsymbol{\alpha}} \boldsymbol{a}_L^{(p)} \| \varepsilon_f \kappa_f \rangle. \quad (11)$$

The same matrix elements appeared in our previous investigation [21] of the double-differential cross section and polarization correlations of atomic bremsstrahlung. The method of their numerical calculation is described in detail in Refs. [21,25], so we only briefly sketch it here. The continuum-state Dirac wave functions were obtained by solving the Dirac equation with a central potential $V_{\rm scr}(r)$ with the help of the RADIAL package by Salvat *et al.* [26]. The effective potential of the neutral atom was constructed as a sum of the (extended-size) nuclear potential $V_{\rm nuc}$ and the potential generated by the electron density,

$$V_{\rm scr}(r) = V_{\rm nuc}(r) + \alpha \int_0^{R_0} dr' \, \frac{1}{\max(r,r')} \, \varrho(r'), \quad (12)$$

where $\varrho(r)$ is the radial electron density of all atomic orbitals and R_0 is the radius of the atom. The electron density was obtained by solving the Dirac-Fock equation for the ground state of the neutral atom.

The radial integrals with the continuum-state Dirac wave functions were evaluated numerically. The whole interval $r \in (0,\infty)$ was divided into two parts, $(0,R_0)$ and (R_0,∞). In the first interval $(0,R_0)$, the integration is performed straightforwardly by dividing the interval into a suitable large number of subintervals and by applying Gauss-Legendre quadratures. In the second interval (R_0,∞), the atomic potential vanishes and the solutions of the Dirac equation turn into the free Dirac solutions. We evaluate the integrals in this region by rotating the integration contour in the complex r plane with the help of the method described in detail in the appendix of Ref. [21].

IV. RESULTS AND DISCUSSION

A. Differential bremsstrahlung cross section

In recent decades, the triple-differential bremsstrahlung cross section has been measured in several experiments [10,11,28]. In these experiments, among other things, the angular distribution of bremsstrahlung was studied as a function of the photon emission angle. The electron scattering angle was held fixed and the photon energy was chosen far from the tip region. In Fig. 2, we display the experimental findings for the radiative scattering of unpolarized 180 keV electrons on silver atoms [10]. In this experiment, the scattered electrons with an energy of 100 keV were detected under the angle $\theta_p = 30^\circ$ and $\varphi_p = 0^\circ$. In order to examine the performance of our theoretical approach, we calculated the triple-differential cross section for these parameters. The result of our calculation is also shown in Fig. 2 and compared,

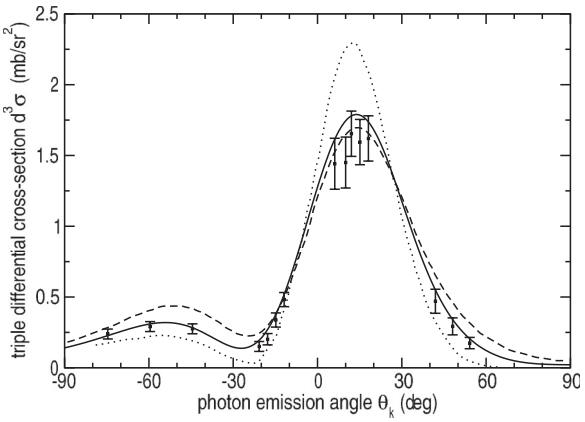

FIG. 2. Scaled triple-differential bremsstrahlung cross section (7) as a function of the photon emission angle θ_k. The calculations have been performed for the scattering of initially unpolarized electrons on neutral silver atoms, for the initial and final electron energies $\varepsilon_i = 180$ keV and $\varepsilon_f = 100$ keV and the fixed electron scattering angles $\varphi_p = 0^\circ$ and $\theta_p = 30^\circ$. Our predictions (solid line) are compared to the calculations of Tseng [16] (dashed line) and Shaffer *et al.* [15] (dotted line). The experimental results are from Aehlig and Scheer [10] (solid squares).

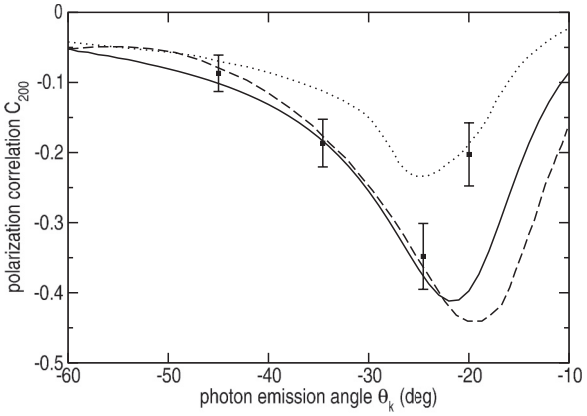

FIG. 3. Polarization correlation C_{200} as a function of the photon emission angle θ_k for the scattering of 300 keV electrons on a gold target. The outgoing electrons with an energy of $\varepsilon_f = 200$ keV were detected under the angles $\varphi_p = 0^\circ$ and $\theta_p = 45^\circ$. Our predictions (solid line) are compared with the results by Tseng [16] (dashed line), Haug [27] (dotted line), and the experiment by Mergl *et al.* [12] (solid squares).

moreover, with previous theoretical predictions [15,16]. As seen from the figure, our predictions reproduce the measurement over the entire angular range. However, obtained using the same partial-wave expansion, the calculations performed by Tseng [16] and Shaffer *et al.* [15] show some discrepancy with the experimental values and our results. This difference might be caused by a convergence problem in the calculations of Shaffer *et al.*, as it was mentioned in Ref. [16], and a different description of the atomic potential. Shaffer *et al.* used a modified version of the self-consistent field program by Liberman *et al.* [29], and Tseng, very similarly, applied the full Kohn-Sham potential [30]. In contrast to that, we obtained the potential of the neutral atom, as discussed in Sec. III C. Moreover, about 40 partial waves were taken into account to get the convergence under control.

The calculations for Fig. 2 were carried our for an unpolarized incident electron beam. During the last decade, however, a new generation of bremsstrahlung experiments with polarized electrons became feasible. These experiments focused on electrons polarized perpendicularly to the emission plane [$\boldsymbol{P}_e = (0,1,0)$]. It follows from the symmetry of the statistical tensor (3) that a perpendicular polarization may affect the angular distribution of bremsstrahlung [21]. In order to quantify the influence of the initial electron polarization, one usually introduces the *emission anisotropy* C_{200} [2]. It is defined by the ratio

$$C_{200} = \frac{d^3\sigma(0,1,0)}{d^3\sigma(0,0,0)} - 1, \tag{13}$$

where the $d^3\sigma(P_x, P_y, P_z)$ are the cross sections for different electron polarizations $\boldsymbol{P}_e$. A measurement of the parameter C_{200} was reported by Mergl *et al.* [12] for the scattering of 300 keV electrons on gold atoms. These results for an electron scattering angle of $\theta_p = 45^\circ$, $\varphi_p = 0^\circ$ and a photon energy of 100 keV are shown in Fig. 3, together with former theoretical predictions by Tseng [16] and Haug [27] and our findings. As seen from the figure, our calculations, based on Eqs. (4)–(6), are in good agreement with the experimental data, except for $\theta_k = 20^\circ$. For this particular angle, the theory of Haug involving Sommerfeld-Maue wave functions gives the best description even though it fails in the range $-40^\circ < \theta_k < -25^\circ$.

Up to now, we discussed scenarios which have been investigated before both in theory and experiment. In these scenarios, the angular distribution of bremsstrahlung radiation was studied for either polarized or unpolarized incident electrons. Applied to these exemplary cases, our theory exhibits a good performance. In the next section, we will use our theory [Eqs. (4)–(9)] to analyze the polarization properties of atomic bremsstrahlung which can be measured in coincidence studies.

B. Polarization of bremsstrahlung photons

1. *Scattering of unpolarized electrons*

The degree of linear polarization P_L of bremsstrahlung was observed in a number of experiments where the scattered electrons remained unobserved [31–33]. These experiments and theoretical calculations [21,34] showed that P_L does not vanish even if the incident electrons are not polarized. In order to investigate how P_L and the polarization angle χ change if the scattered electrons are detected in coincidence with the emitted photons, we performed detailed calculations for the scattering of unpolarized electrons with an initial energy of 100 keV on gold atoms. In Fig. 4, we show our results for P_L (upper panel) and χ (lower panel) for selected electron scattering angles (θ_p,φ_p) and a photon energy of 99 keV. Since our calculations show that the bremsstrahlung yield is increased for large polar electron scattering angles, we present results for $\theta_p = 180^\circ$ (solid line), $\theta_p = 135^\circ$ (dashed line), and $\theta_p = 90^\circ$ (dash-dotted line). For comparison, we show in Fig. 4 predictions assuming a setup where the scattered electrons remain unobserved (dotted line). These *integrated*

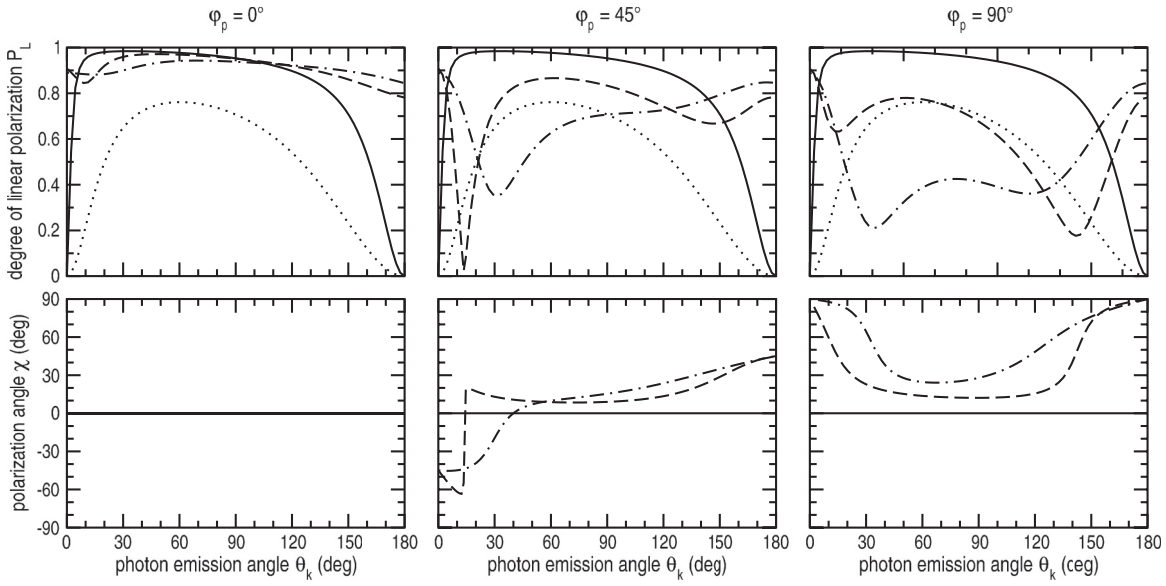

FIG. 4. Degree of linear polarization P_L (upper row) and polarization angle χ (lower row) of bremsstrahlung radiation as a function of the photon emission angle θ_k for three different azimuthal scattering angles $\varphi_p = 0^\circ$ (left column), $\varphi_p = 45^\circ$ (center column), and $\varphi_p = 90^\circ$ (right column) of the electron. The calculations were performed for initially unpolarized electrons, $Z = 79$, an initial electron energy $\varepsilon_i = 100$ keV, a final electron energy $\varepsilon_f = 1$ keV, and polar electron scattering angles of $\theta_p = 180^\circ$ (solid line), $\theta_p = 135^\circ$ (dashed line), and $\theta_p = 90^\circ$ (dash-dotted line). For comparison, we also present the results obtained for the scenarios where the scattered electron is not observed (dotted line).

results are naturally obtained by integrating (4) over the electron scattering angle $\Omega_p = (\theta_p, \varphi_p)$.

As seen from Fig. 4, the degree of linear polarization P_L behaves qualitatively similar for electron backscattering ($\theta_p = 180^\circ$) and after integration over Ω_p. In both cases, P_L vanishes identically for forward ($\theta_k = 0^\circ$) and backward ($\theta_k = 180^\circ$) emission of the photon, while it reaches large values for $20^\circ < \theta_k < 120^\circ$. This behavior can be understood from the symmetry of the bremsstrahlung process. In the geometry where $\theta_p = 180^\circ$, the initial and final electron momenta $\boldsymbol{p}_i$ and $\boldsymbol{p}_f$ are antiparallel. Thus the scattering plane held by these two momenta is not defined and the polarization properties of bremsstrahlung are independent on the azimuthal angle φ_p. If, secondarily, the photons are emitted parallel or antiparallel to the z axis, then the overall system "photon electron" possesses an axial symmetry. Therefore, there is no plane with respect to which one can define the polarization of the bremsstrahlung photons and $P_L = 0$. However, for scattering angles $\theta_p < 180^\circ$, the scattering plane is uniquely defined by $\boldsymbol{p}_i$ and $\boldsymbol{p}_f$ and the axial symmetry of the system is broken. This leads to the fact that for these angles, P_L does not vanish even for forward or backward emission of the photons. For the detection of the scattered electron under the angles $\theta_p = 90^\circ$ and $\varphi_p = 0$, for example, the degree of linear polarization P_L is greater than 80% over the entire angular range $0^\circ \leqslant \theta_k \leqslant 180^\circ$.

As already mentioned in Sec. III, the polarization of bremsstrahlung is characterized by its degree and also by the polarization angle χ. In the bottom panel of Fig. 4, we present results for this angle obtained for the same parameters used for the analysis of the degree of linear polarization P_L. As seen from the figure, the behavior of χ strongly depends on the azimuthal scattering angle φ_p. For instance, it vanishes identically for coplanar emission of the photons and the electrons, i.e., $\varphi_p = 0^\circ$. This behavior, which also resembles the integrated case, is a consequence of the fact that for unpolarized electrons and coplanar emission, the overall system possesses a symmetry with respect to the xz plane. This symmetry would be broken by a nonzero polarization angle χ, so it is zero identically in that case. It is evident that the same arguments hold for the integrated case and nonzero azimuthal scattering angles φ_p, but $\theta_p = 180^\circ$. In contrast, the scattering in a general, noncoplanar geometry leads to nonzero polarization angles which can become very large. As seen from the center column of Fig. 4, for example, the polarization angle can vary from almost -80° to 80° for different photon emission angles and for $\theta_p = 135^\circ$, $\varphi_p = 45^\circ$. This shows clearly, in light of the identically vanishing integrated χ, that the detection of the scattered electron in a $(e,e'\gamma)$ coincidence study can drastically affect the polarization properties of bremsstrahlung radiation.

2. *Scattering of polarized electrons*

In the previous section, we have discussed the linear polarization of bremsstrahlung radiation in $(e,e'\gamma)$ coincidence experiments with initially unpolarized electrons. As already mentioned in Sec. IV A, high-energy scattering experiments with polarized electron beams are nowadays also possible. In recent years, a number of bremsstrahlung measurements with initially polarized electron beams was performed [8,9]. The analysis of these measurements revealed a strong sensitivity of the bremsstrahlung polarization on the spin (polarization) state of the incident electrons. However, all of these experiments left the scattered electrons unobserved. In order to analyze how its detection will affect the behavior of the degree of linear polarization P_L and the polarization angle χ of

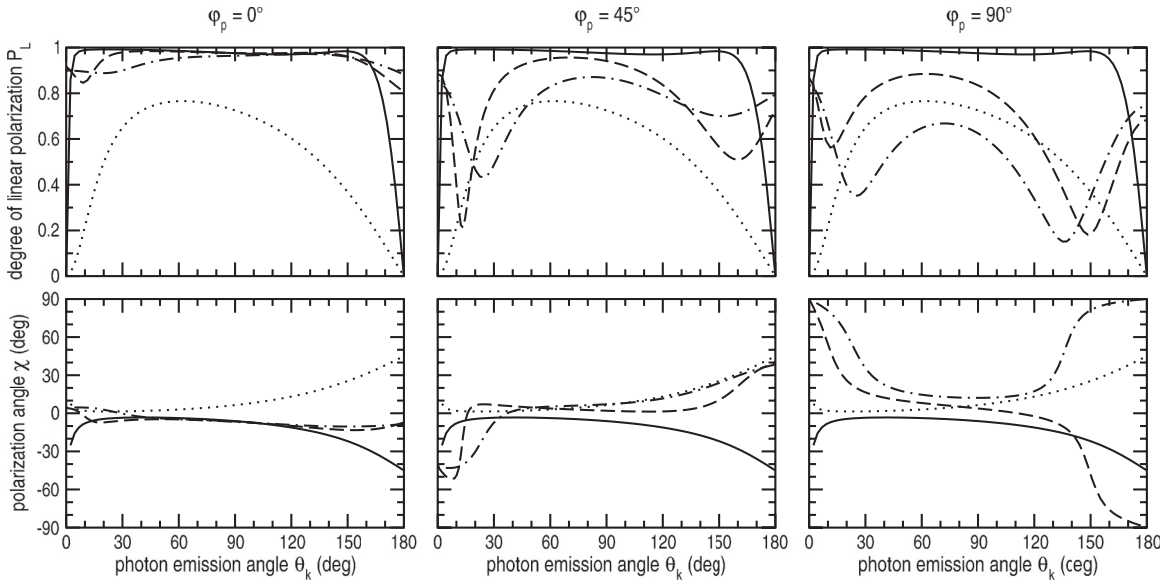

FIG. 5. Degree of linear polarization P_L (upper row) and polarization angle χ (lower row) of bremsstrahlung radiation as a function of the photon emission angle θ_k for three different azimuthal scattering angles $\varphi_p = 0^\circ$ (left column), $\varphi_p = 45^\circ$ (center column), and $\varphi_p = 90^\circ$ (right column) of the electron. The calculations were performed for electrons polarized perpendicularly within the emission plane [$\boldsymbol{P}_e = (1,0,0)$], $Z = 79$, an initial electron energy $\varepsilon_i = 100$ keV, a final electron energy $\varepsilon_f = 1$ keV, and polar electron scattering angles of $\theta_p = 180^\circ$ (solid line), $\theta_p = 135^\circ$ (dashed line), and $\theta_p = 90^\circ$ (dash-dotted line). For comparison, we also present the results obtained for the scenarios where the scattered electron is not observed (dotted line).

bremsstrahlung, we investigate the scattering of electrons, polarized transversally within the emission plane [$\boldsymbol{P}_e = (1,0,0)$] on gold atoms. Similarly to before, we carried out calculations for an incident electron energy $\varepsilon_i = 100$ keV and for several scattering angles $\Omega_p = (\theta_p,\varphi_p)$. As seen from Fig. 5, both P_L and χ are very sensitive to the azimuthal scattering angle φ_p. In particular, for $\varphi_p = 90^\circ$ and a polar scattering angle of $\theta_p = 90^\circ$, the degree of linear polarization P_L becomes smaller than the integrated results in a wide range of photon emission angles $20^\circ < \theta_k < 150^\circ$, while in the same interval but for coplanar scattering, $\varphi_p = 0$, P_L is greater than 80% for all polar scattering angles θ_p. In this scenario, the degree of linear polarization is much larger than P_L obtained under the assumption that the scattered electrons remain unobserved (dotted line). In contrast, the polarization angle χ is reduced if the outgoing electrons are detected under particular angles. For $\theta_p = 90^\circ$ and $\varphi_p = 0^\circ$, for example, χ does not exceed 11°, while it can reach 40° for the integrated case.

In our previous discussions, we always assumed that besides the scattering angle, the energy of the incoming and outgoing electrons was fixed. However, in a recent study by Märtin *et al.* [9], the energy dependence of the polarization angle χ was investigated experimentally. These measurements have been performed for the scattering of 100 keV electrons, polarized transversally within the reaction plane [$\boldsymbol{P}_e = (1,0,0)$] and scattered on a gold target. It was shown that the polarization angle χ does not vanish even if the scattered electrons remain unobserved, which is also reflected in Fig. 6. This is due to the fact that the initial axial symmetry of the system (cf. Sec. IV B 1) is broken by the electron polarization. Moreover, it was found that the polarization angle is only weakly dependent on the amount of energy transferred from the incident electron to the photon. In order to investigate whether such an invariance of the polarization angle also holds for the polarization detected in $(e,e'\gamma)$ coincidence bremsstrahlung experiments, we calculated χ for three electron scattering angles θ_p in a coplanar geometry, $\varphi_p = 0$, and the same parameters used in the experiment in Ref. [9], i.e., $\theta_k = 130^\circ$ and a relative photon energy range $0.7 < \varepsilon_k/\varepsilon_i < 0.99$. The results obtained are presented in Fig. 6. As seen from the figure, the polarization angle χ appears to be strongly dependent on the photon energy if measured in coincidence with the scattered electrons. This becomes most

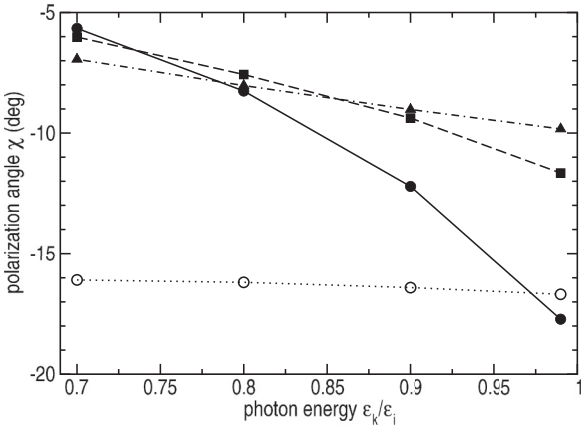

FIG. 6. Polarization angle χ for different photon energies. The calculations were performed for $\boldsymbol{P}_e = (1,0,0)$, $Z = 79$, and initial electron energy $\varepsilon_i = 100$ keV, photon scattering angle $\theta_k = 130^\circ$, and electron scattering angles of $\theta_p = 30^\circ$ (solid circles, solid line), $\theta_p = 60^\circ$ (solid squares, dashed line), and $\theta_p = 90^\circ$ (solid triangles, dash-dotted line) with $\varphi_p = 0^\circ$ always. For comparison, the results $-\chi$ after integration over Ω_p are shown (open circles, dotted line).

evident for $\theta_p = 30^\circ$. Here the absolute value of χ increases by a factor of three if the energy changes from the tip region, where $\varepsilon_k/\varepsilon_i \sim 1$, to softer energies.

V. SUMMARY

In summary, we presented a theoretical study of atomic bremsstrahlung with a special emphasis on the linear polarization of the emitted photons if measured in coincidence with the scattered electrons whose spin states remain unobserved. In order to perform such a $(e,e'\gamma)$ coincidence analysis, we applied the density matrix approach and first-order perturbation theory. Based on the developed approach, detailed calculations have been carried out for the scattering of unpolarized as well as transversally polarized electrons with the initial energy $\varepsilon_i = 100$ keV scattered on gold atoms. These predictions were compared with the integrated results, obtained under the assumption that the scattered electrons are not observed. From this comparison, we found that the detection of the outgoing electrons can drastically affect the polarization properties of bremsstrahlung radiation. For example, strong enhancement of the polarization angle χ can be observed in coincidence studies, even if the incident electrons are unpolarized. Besides the direction, the degree of linear polarization P_L is also very sensitive to the geometry of the coincidence $(e,e'\gamma)$ study. For the coplanar case, for example, P_L is usually much higher than the one obtained in setups where only the emitted photon is detected. The effects predicted in the present work can be observed with the help of available sources and detectors. These measurements will reveal more information about the dynamics of the electron spin as well as electron-photon coupling in the relativistic regime.

ACKNOWLEDGMENTS

The authors are grateful to Dr. R. Märtin, Dr. G. Weber, and Professor S. Hagmann for valuable discussions. R.A.M. acknowledges support of the Studienstiftung des Deutschen Volkes. The work reported in this paper was supported by the Helmholtz Gemeinschaft (Nachwuchsgruppe VH-NG-421).

[1] H. K. Tseng and R. H. Pratt, Phys. Rev. A **3**, 100 (1971).
[2] H. K. Tseng and R. H. Pratt, Phys. Rev. A **7**, 1502 (1973).
[3] J. W. Motz and R. C. Placious, Phys. Rev. **109**, 235 (1958).
[4] D. H. Jakubassa-Amundsen and A. Surzhykov, Eur. Phys. J. D **62**, 177 (2011).
[5] S. Tashenov, T. Bäck, R. Barday, B. Cederwall, J. Enders, A. Khaplanov, Y. Fritzsche, K.-U. Schässburger, A. Surzhykov, V. A. Yerokhin, and D. Jakubassa-Amundsen, Phys. Rev. A **87**, 022707 (2013).
[6] S. Tashenov, T. Bäck, R. Barday, B. Cederwall, J. Enders, A. Khaplanov, Y. Fritzsche, K.-U. Schässburger, A. Surzhykov, and V. A. Yerokhin, Phys. Scr. **T156**, 014071 (2013).
[7] D. H. Jakubassa-Amundsen, J. Phys. B **40**, 2719 (2007).
[8] S. Tashenov, T. Bäck, R. Barday, B. Cederwall, J. Enders, A. Khaplanov, Y. Poltoratska, K.-U. Schässburger, and A. Surzhykov, Phys. Rev. Lett. **107**, 173201 (2011).
[9] R. Märtin *et al.*, Phys. Rev. Lett. **108**, 264801 (2012).
[10] A. Aehlig and M. Scheer, Z. Phys. **250**, 235 (1972).
[11] A. Aehlig, L. Metzger, and M. Scheer, Z. Phys. A **281**, 205 (1977).
[12] E. Mergl, H.-T. Prinz, C. D. Schröter, and W. Nakel, Phys. Rev. Lett. **69**, 901 (1992).
[13] W. Nakel, Phys. Rep. **243**, 317 (1994).
[14] S. Keller and R. M. Dreizler, J. Phys. B **30**, 3257 (1997).
[15] C. D. Shaffer, X.-M. Tong, and R. H. Pratt, Phys. Rev. A **53**, 4158 (1996).
[16] H. K. Tseng, J. Phys. B **35**, 1129 (2002).
[17] G. Weber, H. Bräuning, S. Hess, R. Märtin, U. Spillmann, and T. Stöhlker, J. Inst. **5**, C07010 (2010).
[18] U. Spillmann, H. Brauning, S. Hess, H. Beyer, T. Stohlker, J.-C. Dousse, D. Protic, and T. Krings, Rev. Sci. Instrum. **79**, 083101 (2008).
[19] S. Tashenov *et al.*, Phys. Rev. Lett. **97**, 223202 (2006).
[20] P.-M. Hillenbrand *et al.*, Phys. Rev. A **90**, 022707 (2014).
[21] V. A. Yerokhin and A. Surzhykov, Phys. Rev. A **82**, 062702 (2010).
[22] V. V. Balashov, N. M. Kabachnik, and A. N. Grum-Grzhimailo, *Polarization and Correlation Phenomena in Atomic Collisions: A Practical Theory Course*, Physics of Atoms and Molecules (Springer, Berlin, 2000).
[23] J. Eichler and W. E. Meyerhof, *Relativistic Atomic Collisions* (Academic, New York, 1995).
[24] M. E. Rose, *Elementary Theory of Angular Momentum* (Dover, New York, 1995).
[25] V. A. Yerokhin, A. Surzhykov, R. Märtin, S. Tashenov, and G. Weber, Phys. Rev. A **86**, 032708 (2012).
[26] F. Salvat, J. Fernndez-Varea, and W. Williamson, Comput. Phys. Commun. **90**, 151 (1995).
[27] E. Haug, Z. Phys. D **37**, 9 (1996).
[28] M. Komma and W. Nakel, J. Phys. B **15**, 1433 (1982).
[29] D. A. Liberman, D. T. Cromer, and J. T. Waber, Comput. Phys. Commun. **2**, 107 (1971).
[30] W. Kohn and L. J. Sham, Phys. Rev. **140**, A1133 (1965).
[31] W. Lichtenberg, A. Przybylski, and M. Scheer, Phys. Rev. A **11**, 480 (1975).
[32] H.-H. Behncke and W. Nakel, Phys. Rev. A **17**, 1679 (1978).
[33] W. Bleier and W. Nakel, Phys. Rev. A **30**, 607 (1984).
[34] R. Gluckstern, M. Hull, and G. Breit, Phys. Rev. **90**, 1026 (1953).